ISACoT: Integrating Sensing with Data Traffic for Ubiquitous IoT Devices

Zhe Chen, Tianyue Zheng, Chao Hu, Hangcheng Cao, Yanbing Yang, Hongbo Jiang, Jun Luo

***Abstract*—The intention of leveraging Radio-Frequency (RF) resources for diverse sensing purposes has grown increasingly keen, thanks to the ever-expanding deployment of IoT devices using RF communications to maintain connectivity. Whereas the original idea was to *integrate sensing and communications* (a.k.a. ISAC) for individual IoT devices, most proposals in the past decade simply converted such devices (e.g., Wi-Fi or LoRa) into RF sensors without attending to their communication nature. Therefore, we argue that the device architecture has to be overhauled so as to achieve the ISAC ambition.**

To this end, we propose ISACoT as the framework for enabling ISAC over IoT devices. We categorize ISACoT's extensions over existing devices into four aspects, namely *time*, *frequency*, *space*, and *protocol*. We argue that, as the *multistatic* communication infrastructure of IoT is adverse to *device-free* sensing (e.g., lack of precise time synchronization), the keystone of ISACoT should be operating sensing in a *monostatic* mode (like radar). We tackle the fundamental time aspect based on Wi-Fi first, but leave the other three as challenges for exploration. For each of the three aspects, we present our proposals along with verification experiments, while putting forward challenges along with potential solutions. In particular, the protocol aspect discusses how ISACoT can be generalized to other IoT protocols beyond Wi-Fi.

***Index Terms*—ISAC, IoT, RF sensing, device-free sensing, monostatic sensing, Wi-Fi sensing.**

I. Introduction

Internet of Things (IoT) enables a variety of "things" pervasively presenting around us to interact with each other [1]. Significantly different from the Internet, IoT is not only a data-exchanging network, but also in charge of capturing information by sensing the physical world [1]. Existing IoT often implements the two fundamental functionalities (i.e., sensing and communication) independently: sensors collect data and networks route data. However, the concept of IoT should not be hardened to only "networked sensors", as the *radio-frequency* (RF) communication infrastructure itself has the potential to serve sensing purposes, hence leading to *integrated sensing and communications* (ISAC) solutions [2]. In the following, we first explain the importance of ISAC to IoT, then we critically point out the adverse nature of IoT to ISAC, and we finally summarize our contributions and resulting challenges in this paper.

A. ISAC is Imperative to IoT

While involving specialized sensors as the front-end of IoT might be inevitable, the RF resources substantially leveraged for the (wireless) connectivity in IoT should not be neglected. In fact, *device-free sensing* exploiting a variety of RF communication devices has been heavily studied [3], [4]: though they mostly attempt to use RF signals directly for sensing purposes without attending to the mutual interactions between sensing and communication (thus their integration), they did start to pave the way towards full-fledged ISAC designs for IoT. Meanwhile, many emerging IoT services call for new sensing modalities, and ISAC can cater to such needs without adding extra cost to system construction.

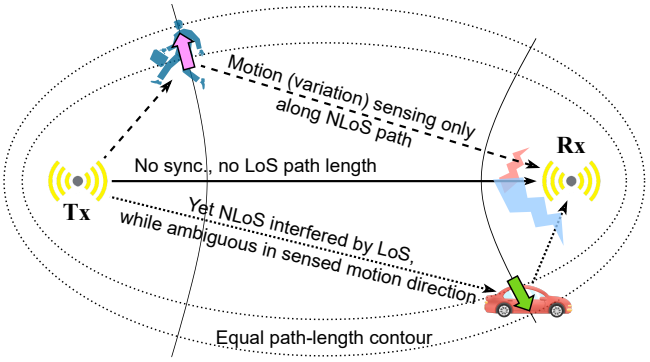

Fig. 1: Multistatic (only bistatic illustrated here for brevity) communication infrastructure is harmful to device-free sensing. The thin arrows represent RF propagation along distinct paths, while the thick (colored) arrows denote the directions of sensed reflector motions.

B. Multistatic is Adverse to Sensing

To enable ISAC, we have to tap into the RF connectivity of spatially separated IoT nodes, which is *multistatic* in nature. However, this multistatic setting is adverse to device-free sensing for three major reasons, as also illustrated in Fig. 1:

a) Inaccurate Ranging due to Asynchrony: IoT often achieves synchronization using protocols with accuracy at the microsecond level. However, these protocols fail to correct nanosecond offsets inherent to different devices not sharing the same clocks and other processing units [5] (e.g., a local oscillator not synchronized with a received carrier causes carrier frequency offset). Since 10 ns implies roughly a 3 m ranging error, the asynchrony of several nanoseconds is intolerable to sensing. This has forced existing device-free proposals (e.g., [3], [6]) to only measure variations along or between the *line-of-sight* (LoS) and *non-line-of-sight* (NLoS) paths.

b) Dominating Interference from LoS Path: In a multistatic IoT network, wireless signals travel from a transmitter to a receiver via both LoS and multiple NLoS paths. Whereas the LoS path mostly carries communication data, NLoS paths are where sensing often happens. However, the LoS signal strength

is much stronger and tends to overwhelm those of NLoS paths: the power difference between LoS and NLoS paths can be up to 67 dB. The dominating LoS interference leads to a high quantization noise in NLoS signals [7], rendering the IoT RF signals less useful for sensing purposes.

c) Ambiguity in Motion Sensing: Motion sensing is another crucial capability of RF signal, as it captures the distance variation of a reflector. Due to the multistatic nature of IoT (illustrated as *bistatic* in Figure 1), distance variations take place along the gradient direction of the Fresnel field [8] whose contours are ellipsoids. However, since the direction of a gradient (tangent to a hyperbola) cannot be determined without knowing the reflector's range information, the sensed variation magnitude can be meaningless as severe ambiguity exists in interpreting motion sensing results.

C. Our Solutions and Potential Challenges

To combat the adverse effects of multistatic IoT, we propose to fundamentally overhaul IoT architecture so that sensing is conducted in *monostatic* mode: the antenna(s) of each IoT node, while transmitting data packets, simultaneously capture the reflected signals induced by these transmissions. Apparently, this overhaul may largely eliminate the adverse effects because i) the transmitter (Tx) and receiver (Rx) are co-located and share the same clock and processing units, ii) LoS interference disappears, and iii) sensed motion direction is well determined by the Tx and reflector. To fulfill these promises, ISACoT is developed to contain a novel RF front-end capable of effectively separating concurrent Tx and Rx signals. While this basic prototype enables a single Wi-Fi device to operate in an ISAC manner, several challenges remain towards a full-fledged ISACoT for all kinds of IoT devices. Therefore, we expand the exploration on ISACoT along the perspectives of *frequency*, *space*, and *protocol*, by stating the challenges and putting forward tentative solutions.

- *Bandwidth Expansion*: Modern IoT spans across multiple frequency bands worthy of being exploited to increase sensing resolution and combat interference.
- *MIMO for ISAC*: The spatial diversity introduced by the MIMO (multiple-input and multiple-output) technology is often utilized to enhance communication performance, so ISACoT needs to leverage MIMO for sensing.
- *Protocol Compatibility*: IoT encompasses a variety of wireless communication protocols, with which ISACoT needs to be integrated, better via a one-size-fits-all design.

The rest of the paper is organized as follows. We discuss the basic ideas of ISACoT in Section II, where we present a preliminary design based on Wi-Fi; it tackles the time-domain challenges to enabling monostatic sensing. In Sections III, IV, and V, we respectively discuss how to expand the capabilities of ISACoT with respect to frequency, space, and protocol, accompanied by brief experiment evaluations. We finally conclude the paper in Section VI.

II. ISACoT for Wi-Fi: A Basic Design

We adopt Wi-Fi to implement our basic ISACoT prototype due to its wide adoption and bountiful development support.

A. Background on Wi-Fi Sensing

Modern Wi-Fi sensing proposals rely on CSI (channel state information) to capture signals propagation from Tx to Rx via distinct carrier frequencies and along multiple paths. Mathematically, CSI (thus the channel) of the k-th subcarrier ($k = 0, \pm1, \pm2, \cdots$) and ℓ-th data packet can be expressed as $H_\ell(k,\tau)$ (see "ideal CSI" on the top of Fig. 2), where M is the path cardinality, $\alpha_{p,\ell}$ and $\tau_{p,\ell}$ denote the amplitude and propagation delay along the p-th path, f_c and Δf represent the centre frequency and subcarrier spacing, respectively. In reality, the asynchrony between bistatic Tx and Rx results in temporal uncertainties, leading to a CSI measurement $H'_\ell(k,\tau)$ with contaminated phases (see "CSI with offsets" in Fig. 2), where γ_c, ϕ_c, β, ϵ denote the CFO (carrier frequency offset), CPO (carrier phase offset), SFO (sampling frequency offset), and PDD (packet detection delay), respectively. Though derived for Wi-Fi, these phase offsets apply to most IoT devices given the generic design in RF front-end. Existing device-free sensing under the multistatic mode relies on complicated yet non-robust algorithms to mitigate these uncertainties [6], [3]. Fortunately, switching to the monostatic design that co-locates the Tx and Rx for sensing would naturally solve the synchronization issue, thus retaining the idea CSI $H_\ell(k,\tau)$. It is worth noting that, as CPO is caused by the random initialization phase, it can be changed by resetting a device and hence requires a specific calibration; we shall revisit CPO when discussing channel hopping later.

B. Challenges to Monostatic Wi-Fi Sensing

Though adopting monostatic sensing addresses all major problems incurred by multistatic sensing, the cost of removing the LoS-interference indicated by $p = 1$ in $H_\ell(k,\tau)$ is the newly appeared Tx-interference represented by $p = 0$; it was avoided for communications by the temporal separation imposed by protocol. As a naive solution, *full duplex radios* (FDR) [9] is trained under a "quiet" situation (no incoming transmissions) so that the Rx signal $R(k,\tau) = H(k,\tau)S(k)$ is purely induced by the Tx signal $S(k)$; it aims to generate a cancelling CSI H_C (both analog and digital) so as to eliminate $R(k,\tau)$, by minimizing $Z(k,\tau)$ shown in Fig. 2 for "FDR". Unfortunately, this FDR design does not work for monostatic sensing. The reason is that, whereas the 0-th component of $H(k,\tau)$ needs to be removed, the remaining (multipath reflection) components ($p > 1$) are crucial to monostatic sensing. To illustrate this challenge, we let a pendulum swing along the radial direction of ISACoT and show the performance of the FDR cancellation in Fig. 2 under the "FDR" scenario. As illustrated by both the blue and orange curves in the upper figure, turning off the cancellation from 0 s to 10 s severely corrupts the signal variation caused by the swinging pendulum. Although the Tx-interference is well suppressed under the noise floor from 10 s to 20 s by turning on the FDR cancellation, the desired signal variation also vanishes.

C. Tx-Interference Removal for ISACoT

Our key design for ISACoT is a *Tx-Rx separator* shown in Fig. 2 on the "ISACoT" panel. Inspired by [9], this

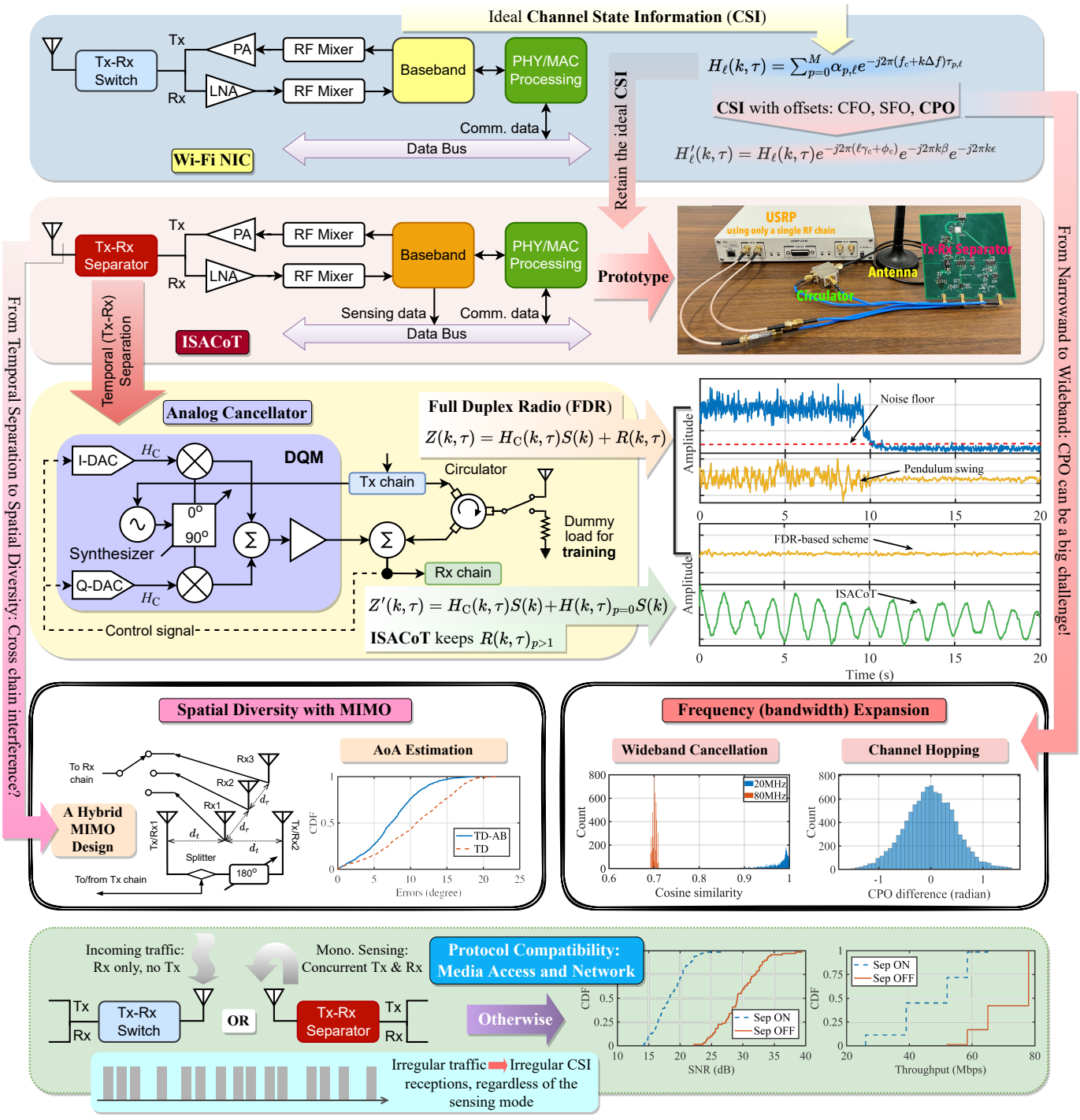

Fig. 2: Time, frequency, spatial, protocol aspects of ISACoT.

separator contains both analog and digital cancellators. We first introduce the basic principle behind these cancellators, then we discuss their detailed constructions. Different from FDR, our separators aim to minimize $Z'(k,\tau)$ (shown on the "Analog Cancellator" panel of Fig. 2) containing only the 0-th component of $R(k,\tau)$ but to retain other multipath components $R(k,\tau)_{p>1}$, achieved by adding a switch to toggle between an antenna and a dummy load (illustrated on the same panel), so as to train the separator under an even "quieter" situation free of $R(k,\tau)_{p>1}$ in $Z(k,\tau)$ by switching to the dummy load.

We adopt a *direct quadrature modulator* (DQM) to realize the *analog cancellator*. This much simpler yet more effective architecture is trained to approximate the inverse of $H(k,\tau)_{p=0}$ (comprised of the internal propagation path within the RF front-end) given the dummy load, and it can thus minimize only $Z'(k,\tau)$ during concurrent transmissions and monostatic sensing. Since we cannot change the design of existing Wi-Fi NICs, our ISACoT prototype is built over USRP X310, as shown by "Prototype" in Fig. 2 (on the "ISACoT" panel); it further contains a general purpose I/O controller (integrated

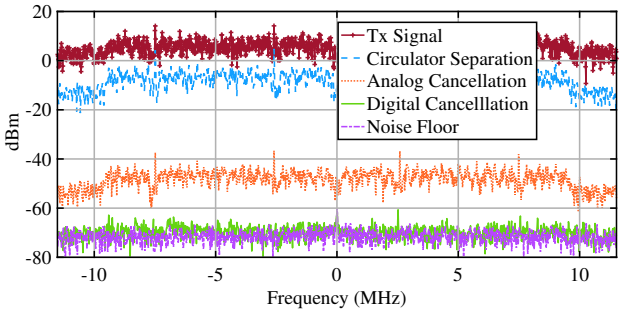

Fig. 3: Power spectrum of the received baseband signal after various components of Tx-Rx separators.

into the analog cancellator board) to toggle an RF switch between the antenna and dummy load. Basically, signals from antennas are first fed to a circulator to roughly split Tx and Rx, then the outcome is taken by the analog cancellator to filter the Tx-interference. Though the output may still have residue Tx-interference, the dynamic range has been significantly reduced to the level that sampling it with the ADC of the USRP results in neither saturation nor large quantization errors. Consequently, the samples are taken by a *digital cancellator* (programmed to run by the USRP) to further cleanse the Tx-interference. Though sharing the same principle as its analog counterpart, the digital cancellator differs in that H_C is trained as an adaptive filter whose coefficients are obtained via an LMS (least mean squares) algorithm. As shown in Fig. 2 (by the lower figure on the right side of the "Analog Cancellator" panel), our ISACoT clearly captures the pendulum swinging process (the green curve) while the FDR-based scheme (the orange curve) totally fails.

D. Microbenchmarking on ISACoT

We hereby report a few key evaluation results for benchmarking the basic functions of ISACoT. We first depict the performance of Tx-Rx separation with the Tx power set to 5 dBm in Fig. 3. It can be observed that, while the circulator results in a 12dB reduction, the analog and digital cancellators further reduce the Tx-interference by 40 dB and 25 dB, respectively. The total cancellation brings the residue Tx-interference very close to the noise floor. To demonstrate the ranging and motion sensing performance of ISACoT, we take USRP without our Tx-Rx separator as the baseline, and we adopt the MUSIC algorithm [10] for parameter estimations. We fix a metal cylinder (radius 0.1 m and height 1.2 m) on a robot car and control the car remotely to move from 1 m to 15 m, with a 1 m step size in a corridor and a speed ranging from 0.6 m/s to 3.5 m/s. We obtain the ranging and speed errors shown in Fig. 4a and 4b: the median ranging errors are 2.84 m and 14.14 m for ISACoT and the baseline, while median speed errors are 0.37 m/s and 1.92 m/s. Whereas the advantage of our separator is evident, the MUSIC algorithm cannot make the best out of our design, for the reason to be elaborated later.

III. Frequency: Ultra-Wideband

Existing radar-based sensing platform leverages an ultra-wide bandwidth to achieve centimeter-level range resolution [11], but IoT devices do not enjoy such a luxury. Given

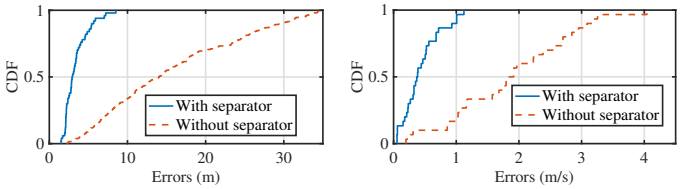

(a) Ranging errors. (b) Speed errors.

Fig. 4: Ranging (a) and motion sensing (b) error comparisons between ISACoT and a baseline.

our basic prototype, we explain the challenges and potential solutions to expand ISACoT's operating frequency range.

A. Challenges to Ultra-Wideband Sensing

We hereby discuss the challenges faced by two potential solutions aiming to extend ISACoT towards ultra-wideband.

a) Direct Wideband Cancellation: Given the increasing bandwidth provided by new generations of Wi-Fi, one may naturally expect to adapt our Tx-Rx separator to a wider bandwidth. However, as frequency response cannot remain perfectly flat and time-invariant within a given frequency band, increasing bandwidth simply exacerbates the situation. We study the stability of Tx-interference, under 20 MHz and 80 MHz bandwidth respectively, by computing the cosine similarity among all received CSIs. We use the ISACoT prototype to transmit 10,000 packets but bypassing the separator; the resulted cosine similarity histograms are shown in Fig. 2 ("Wideband Cancellation" on the "Frequency Expansion" panel); they clearly demonstrate that the wider bandwidth (only 80 MHz, not even ultra-wideband) causes much serious deviations among CSIs received at different times. Consequently, cancelling the Tx-interference for wideband entails much more expensive hardware, violating the "frugality" principle of our ISACoT design.

b) Channel Hopping with Sub-band Cancellation: As IoT devices all adopt contention-based channel access, individual devices should occupy a narrow bandwidth to avoid causing unnecessary contentions. In reality, it is still sensible for Wi-Fi to adopt 20 MHz bandwidth even when wider bandwidth becomes available. Therefore, channel hopping appears to be a more reasonable choice for sampling a wide bandwidth, but it faces another challenge in practice. Recalling that the CPO ϕ_c in $H'_\ell(k,\tau)$ cannot be tackled by monostatic sensing. To verify our statements, we conduct an experiment where we use a fixed-length RF coaxial to connect Tx and Rx chains in USRP and hop to the different carrier frequencies; the histogram of resulted CPO variations shown in Fig. 2 ("Channel Hopping" on the "Frequency Expansion" panel) indicates a truncated zero-mean normal distribution (between $-\pi/2$ and $\pi/2$). This randomness can be attributed to the PLL's behavior in unlocking-locking the local oscillator before and after a channel hopping.

B. Generalized Ranging Approach

Weighting up the aforementioned challenges, we tentatively decide to leverage channel hopping for bandwidth expansion,

by rising to the challenge of calibrating CPOs. In addition, relying on continuous channel hopping is nearly impossible in practice, because certain channels may not be available when in need. Consequently, our general ranging approach aims to sample discontinuous but idle channels.

a) CPO Calibration under Channel Hopping: To calibrate the CPOs caused by channel hopping, we consider two main components in the CSI phase of the i-th channel: physical channel delay and CPO ϕ_c^i. The commonly adopted method to calibrate CPO involves a "short circuit" between Tx and Rx chains (before antennas) controlled by two switches: as the propagation delay via this circuit is designed to be known, switching both chains to this circuit allows for the deduction of ϕ_c^i. Since this design substantially complicates the hardware, we propose to leverage a *two-way* transmission along the circuit to cancel the unknown propagation delay. Basically, after each channel hopping, both Tx and Rx chains are toggled to the circuit and then they transmit to each other. Subtracting the CSI phase of one chain from that of another chain should give us the doubled ϕ_c^i value.

b) Sparse Recovery for Non-Continuous Channels: After the CPO calibration, we obtain a *CSI tensor* $H_\ell(i,k,\tau)$ whose individual components $H_\ell(k,\tau)$ are CSI matrices for respective channels. To estimate parameters such as the delay $\tau_{p,\ell}$ under discontinuous channels, we formulate the problem as a sparse optimization with the L_1 norm of the parameter vector as the objective and the constrain being an over-determined equation system that equalizes $H_\ell(i,k,\tau)$ with an ideally reconstructed channel template. We conduct experiments to validate these solutions using earlier settings, with 10 arbitrary 20 Mhz channels in the range from 5.160 GHz to 5.885 GHz for ISACoT and MUSIC again adopted as the baseline. The results illustrated in Fig. 5a show median errors of 0.41 m and 0.95 m respectively for ISACoT with and without calibration (resp. wc and woc), while that of the baseline (0.65 m) is worse than ISACoT-wc, because our algorithm refines its estimation with multiple iterations. We also show the performance improvement of ISACoT-wc while increasing channel numbers from 1 to 10 in Fig. 5b.

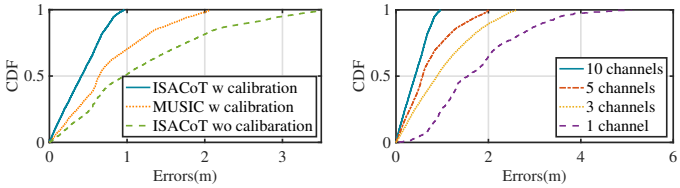

(a) CPO calibration. (b) Number of channels.

Fig. 5: Ranging performance of wideband sensing.

IV. Space: MIMO Sensing

Acquiring a finer spatial resolution demands MIMO sensing with multiple antennas, whose design entails a much higher degree of freedom, hence offering more opportunities.

A. Approaching ISAC-MIMO

Three major architectures exist to enable ISAC-MIMO, namely time-division, digital beamforming, and analog beamforming [11]. *Time-Division* (TD) MIMO enforces different antennas to be in Tx/Rx states at non-overlapping time slots; it is cheap and easy to implement, but it incurs non-negligible time delays. *Digital Beamforming* (DB) employs multiple RF chains each equipped with a single antenna. It transmits or receives signals simultaneously, and hence has the most flexible and fast beam steering capability. Unfortunately, large-scale DB can be too costly for IoT devices. *Analog Beamforming* (AB) consists of two RF chains (respectively for Tx and Rx similar to TD) each with multiple antennas driven by phase shifters (a.k.a. phased antenna array). It selects different beamforming patterns (via different phase shifter paths) to steer Tx and Rx towards pre-defined directions. Apparently, AB's performance and cost sit between TD and DB, and building high-quality shifters can be nontrivial.

B. A Preliminary TD Implementation

We choose to realize a preliminary ISAC-MIMO implementation based on a hybrid TD-AB architecture with two RF chains: one for Tx while another for pure Rx. Since our separator is calibrated only for internal Tx-interference within a chain circuit, it may not properly handle the interference cancellation across different chains. Consequently, we need an additional mechanism to cancel cross-chain Tx-interference, and we borrow from the phase cancellation idea of a simple AB architecture [12]. As illustrated in Fig. 2 on the "Spatial Diversity with MIMO" panel, the Tx chain retrofits the right side of the circulator of ISACoT to drive two symmetrically placed antennas via a (phase) splitter, and the Rx chain employs a switch to receive from three Rx antennas separated by half wavelength d_r. These five antennas are strategically placed so that the axis of the later three is perpendicular to that of the first two. While the internal Tx-interference is handled by our separator within the Tx chain, the Rx chain experiences a two-stage cancellation: the 180° phase splitter causes the Tx-interference to have a zero sum at the Rx chain, leaving the separator implemented within the Rx chain to handle the residue. We verify the performance of this design by placing a rotary robot 1.5 m from ISACoT with six different bearings: $0°, 30°, 45°, 60°, 75°, 90°$. We apply MUSIC to estimate the AoA (angle of arrival) and compare the two designs with and without the phase splitter. According to the results plotted on the same panel in Fig. 2, it is evident that the simple AB upgrade outperforms the one without it, since the cross-chain interference is better suppressed.

C. Challenges to ISAC-MIMO

Our hybrid TD-AB design is only a taste of ISAC-MIMO; it leaves plenty of challenges for further studies.

a) From Hybrid to AB MIMO: Our preliminary design incurs a technical issue: a target close to the axis of the Rx antennas can barely be detected due to the mutual cancellation of the two Tx signals, and the sensing resolution can be affected by the distance between the target and the axis. While a direct solution to this issue is adopting phased antenna array for the Tx chain to avoid the "dead angle", switching to pure AB MIMO implementation may yield a much better spatial resolution leveraging the beam scanning algorithms used

for mmWave sensing. Nonetheless, how to suppress cross-chain Tx-interference via intelligent beamforming scheduling remains to be a challenge.

b) Aliasing Layout MIMO: Instead of the expensive phased array, specially designed TD antenna layout is much cheaper while avoiding the cross-chain interference by relying on only one RF chain. Consider the equally spaced antennas in our preliminary design, the spacing sequence of the *virtual array* becomes $[0, 2d_r, 2d_r]$. Since this layout leads to aliasing beamforming patterns preventing a target to be distinguished, we upgrade it with a special strategy where the spacing sequence of physical and virtual arrays are respectively set as $[0, d_r/2, d_r]$ and $[0, d_r, 2d_r]$. Consequently, one anti-aliasing and two aliasing beamforming patterns are generated by three antennas pairwisely, thus a target can be detected by combining these patterns. However, this layout may not handle nearby targets with only one anti-aliasing pattern, and it can be too strict for hardware design.

c) Large-scale DB MIMO: If cost is not an issue, large-scale (i.e., more than 10 antennas in an array [13]) DB MIMO can be adopted to deliver high spatial resolution; it may even drop the need for the analog cancellator shown in Fig. 2, by leveraging part of its RF chains (hence antennas) to transmit phase-complementing signals and hence to null the cross-chain Tx-interference at the remaining Rx chains [14]. However, as the Tx-interference is blended with the reflected signals (similar to the FDR situation discussed earlier), DB MIMO may face challenges in acquiring qualified monostatic sensing information. One may argue for a directional beamforming solution to avoid the cross-chain interference (as opposed to the above nulling scheme), yet this virtually degenerates DB to AB; we hence leave a new beamforming algorithm design for DB ISAC-MIMO as another challenge.

V. Towards Generalized ISACoT

We herein discuss two levels of protocol compatibility for ISACoT: i) between sensing and communication and ii) with other IoT protocols beyond Wi-Fi.

A. Communications during Sensing

Although our Tx-Rx separator allows for currently sensing and communication at hardware level, the resulting hardware operations may not be compatible with Wi-Fi at protocol level. As shown on the bottom panel of Fig. 2, applying the Tx-Rx separator during normal packet receptions significantly reduces SNR and hence throughput: because the MAC protocol prohibits Tx from transmitting, the separator is reduced to a noise-driven filter. In fact, it is a waste of computing resource to apply the Tx-Rx separator on normal Rx signals. In addition, as normal Wi-Fi traffic contains a series of irregular packets, the sequence of CSIs contained in the reflected Rx signals are also irregular. As a result, existing Wi-Fi sensing approaches that implicitly assume regular CSI receptions [6], [3] may fail to achieve adequate performance. We conduct experiments again with the rotary robots and 80 MHz bandwidth (with channel hopping): under irregular CSI receptions, the FFT baseline algorithm barely delivers a reasonable resolution due to the dispersed energy, as shown on the upper panel of Fig. 6a.

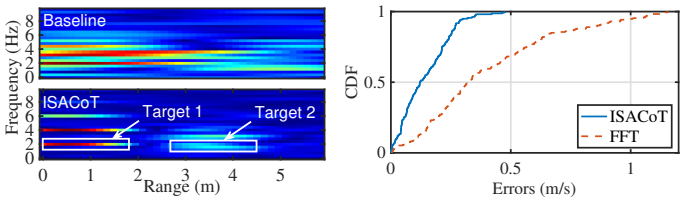

(a) Examples. (b) Speed errors.

Fig. 6: Motion sensing heatmap (a) and error comparisons (b) between ISACoT and FFT baseline.

To avoid interfering normal receptions, we propose and implement a minor yet critical revision to the MAC protocol. In particular, ISACoT starts with a C-state (for communications), and a DATA or ACK message invokes the transition to an M-state (for monostatic sensing), which respectively activates the analog and digital cancellators by a hardware interrupt and a function call. A transition back from the M-state to the C-state is controlled by a timer fine-tunable to suit surrounding environments. As for handling the irregular CSI receptions, we leverage NFFT (non-uniform fast Fourier transform) to enhance the sparse optimization framework introduced earlier. As shown on the bottom panel of Fig. 2, switching off the separator before packet reception does significantly improve the performance of Wi-Fi communications. In addition, our NFFT enhanced sparse optimization enables ISACoT to achieve speed estimation accuracy far more superior to that achieved by the FFT baseline algorithm, as shown in both Fig. 6a (the lower panel) and 6b.

B. ISAC beyond Wi-Fi

The final target of ISACoT is aiming for a general and protocol-free ISAC architecture. Because it is a non-trivial task to tackle all kinds of IoT devices in one paper, we only lay down a few opportunities and challenges.

a) One-Size-Fits-All Design: Though ISACoT is currently designed only Wi-Fi, its plug-and-play and protocol-independent architecture should allow it to be smoothly migrated to other IoT protocols such as Bluetooth, LoRa, Zigbee, NB-IoT, and Sigfox, especially attributed to two major reasons. On one hand, ISACoT only utilizes CSIs for sensing, which are offered by almost all IoT devices in their firmware. On the other hand, the frequency range of ISACoT coincides with most IoT protocols. Interestingly, we also find that certain modulations, e.g., chirp spread spectrum adopted by LoRa, may help improving the Tx-interference suppression, since frequency modulation scheme concentrates energy into a single frequency component at any given point in time, standard low pass filter may be sufficient to handle Tx-interference.

b) Encompassing Other Sensing Modes: In fact, ISACoT does not have to be confined to only monostatic sensing mode; it is certainly compatible with the well-studied multistatic sensing mode [4], [3]. This is because, when bypassing the Tx-interference separator under the C-state, an IoT device simply works under the normal communication mode and multistatic

sensing can directly piggyback on it, while exploiting our proposals on bandwidth expansion and protocol compatibility to improve sensing performance. More importantly, encompassing recent *cross-technology sensing* (CTS) [15] under our ISACoT framework should also be possible, as CTS is by default operating under the multistatic sensing mode. Combining monostatic sensing with multistatic sensing should significantly expand the distributed collaborative sensing involving many IoT devices.

VI. Conclusion

Bearing the ambition of making all IoT devices ISAC-ready, we propose ISACoT as a general framework encompassing time, frequency, space, protocol aspects of the problem. While our preliminary prototype has largely addressed the time-domain aspect of ISACoT under Wi-Fi, we are still on the way to extending it towards wider bandwidth, higher spatial diversity, and broader protocol compatibility. We present our preliminary studies and implementations for each aspect, while leaving a few critical issues as challenges, expecting our research community to join forces in fully tackling them.

References

[1] K. Ashton, "That 'Internet of Things' Thing," *RFID Journal*, vol. 22, no. 7, pp. 97–114, 2009.

[2] Y. Cui *et al.*, "Integrating Sensing and Communications for Ubiquitous IoT: Applications, Trends, and Challenges," *IEEE Network*, vol. 35, no. 5, pp. 158–167, 2021.

[3] K. Qian *et al.*, "Widar2.0: Passive Human Tracking with a Single Wi-Fi Link," in *Proc. of the 16th ACM MobiSys*, 2018, p. 350–361.

[4] W. Jiang *et al.*, "Towards Environment Independent Device Free Human Activity Recognition," in *Proc. of the 24th ACM MobiCom*, 2018, pp. 289–304.

[5] M. Kotaru *et al.*, "SpotFi: Decimeter Level Localization Using WiFi," in *Proc. of 29th ACM SIGCOMM*, 2015, p. 269–282.

[6] J. Wang *et al.*, "LiFS: Low Human-Effort, Device-Free Localization with Fine-Grained Subcarrier Information," in *Proc. of the 22nd ACM MobiCom*, 2016, p. 243–256.

[7] D. C. Halperin, "Simplifying the Configuration of 802.11 Wireless Networks with Effective SNR," *arXiv preprint arXiv:1301.6644*, 2013.

[8] F. Zhang *et al.*, "From Fresnel Diffraction Model to Fine-grained Human Respiration Sensing with Commodity Wi-Fi Devices," in *Proc. of the ACM IMWUT*, 2018, vol. 2, no. 1, pp. 1–23.

[9] D. Bharadia *et al.*, "Full Duplex Radios," in *Proc. of the 27th ACM SIGCOMM*, 2013, pp. 375–386.

[10] R. Schmidt, "Multiple Emitter Location and Signal Parameter Estimation," *IEEE Trans. on Antennas and Propagation*, vol. 34, no. 3, pp. 276–280, 1986.

[11] Z. Chen *et al.*, "Octopus: A Practical and Versatile Wideband MIMO Sensing Platform," in *Proc. of the 27th ACM MobiCom*, 2021, pp. 601–614.

[12] E. Aryafar *et al.*, "MIDU: Enabling MIMO Full Duplex," in *Proc. of the 18th ACM MobiCom*, 2012, pp. 257–268.

[13] Q. Yang *et al.*, "BigStation: Enabling Scalable Real-time Signal Processingin Large MU-MIMO Systems," *ACM SIGCOMM Computer Communication Review*, vol. 43, no. 4, pp. 399–410, 2013.

[14] E. Everett *et al.*, "SoftNull: Many-Antenna Full-duplex Wireless via Digital Beamforming," *IEEE Transactions on Wireless Communications*, vol. 15, no. 12, pp. 8077–8092, 2016.

[15] R. Liu *et al.*, "WiBeacon: Expanding BLE Location-based Services via Wifi," in *Proc. of the 27th ACM MobiCom*, 2021, pp. 83–96.

Zhe Chen (chenz@ssijri.com) is the founder of AIWiSe. He received his PhD with honor in Computer Science from Fudan University, China, with Doctoral Dissertation Award from ACM SIGCOMM China 2019. His research interests include RF communication and sensing systems, deep learning, and IoT applications.

Tianyue Zheng is currently working towards his PhD in Computer Science from Nanyang Technological University (NTU), Singapore. His research interests include RF sensing and deep learning.

Chao Hu is pursuing Master's degree with the College of Computer Science in Sichuan University, China. His research interest include wireless networking, Wi-Fi sensing, and visible light communication.

Hangcheng Cao is a PhD student with the College of Computer Science and Electronic Engineer, Hunan University, China, and he works as a visiting student at NTU from 2021 to 2022. His research interests lie in the area of IoT security and contact-free sensing.

Yanbing Yang received his PhD in Computer Science and Engineering from NTU. He is currently an associate research professor in College of Computer Science, Sichuan University, China. His research interests include visible light communication & sensing and their applications.

Hongbo Jiang received his PhD from Case Western Reserve University, USA. He is now a full professor in the College of Computer Science and Electronic Engineering, Hunan University. His research focuses on computer networking, especially, wireless networks, data science in Internet of Things, and mobile computing.

Jun Luo (junluo@ntu.edu.sg) received his PhD in Computer Science from EPFL, Switzerland. He is currently an associate professor at School of Computer Engineering, NTU. His research interests include mobile/ubiquitous computing, machine learning, and applied operations research.